

When Half Is Better Than the Whole: Advances in Haploid Embryonic Stem Cell Technology

Chikara Kokubu¹ and Junji Takeda^{1,*}

¹Department of Social and Environmental Medicine, Graduate School of Medicine, Osaka University, Suita, Osaka 565-0871, Japan

*Correspondence: takeda@my-envi.med.osaka-u.ac.jp

<http://dx.doi.org/10.1016/j.stem.2014.02.001>

Recent advances in embryonic stem cell (ESC) derivation and genome editing offer efficient platforms for genetic screening. In this issue, Li et al. and Leeb et al., respectively, expand such applications by generating haploid rat ESCs for screening, mutagenesis, and CRISPR-Cas-mediated gene targeting and by developing a forward genetic screen for interrogating haploid mESCs.

In the past three decades, mammalian genetics and stem cell biology have been developed in close synergy with each other. Continuous technological progress in mammalian genetics largely depends on the availability of mouse embryonic stem cells (ESCs). Many reverse genetic approaches have taken advantage of the pluripotency of genetically engineered mouse ESCs to produce animals with germline-transmitted mutations. However, in forward genetic screens, researchers have often employed the self-renewal property of cultured mouse ESCs to streamline mutagenesis and clone archival resources, and in comparison to whole-animal approaches, using mouse ESCs thus offers significant flexibility and cost reduction. If ESC-based genetic approaches are to be extended to a broader range of animal species and applications, two major obstacles should be addressed: low or variable rates of germline transmission in different strains and species and difficulties in phenotype-driven screening of recessive genetic traits that are masked by the diploid nature of mammalian genomes. In this issue of *Cell Stem Cell*, Li et al. (2014) (Figure 1A) and Leeb et al. (2014) (Figure 1B) demonstrate practical solutions to these problems. It is noteworthy that both studies are based on haploid ESC technology.

In mammals, haploidy is normally restricted to the post-meiotic stages of germ cells and represents the end point of cell proliferation, which means that physiological haploidy is incompatible with self-renewal. The recent advent of haploid mouse ESC technologies has drastically changed this situation. The

original versions of haploid ESC lines (Eiling et al., 2011; Leeb and Wutz, 2011) were generated by parthenogenetic activation of unfertilized mouse oocytes with chemicals such as strontium salt or ethanol (Figure 1B). These haploid mouse ESCs contain only the maternal set of chromosomes and show pluripotency as well as self-renewal capabilities. Because these cells show an inherent tendency toward spontaneous diploidization in culture, periodic purification by flow sorting is necessary if cultures containing a large majority of haploid cells are to be maintained. Although haploid ESCs appear to be inevitably diploidized upon differentiation, they can give rise to a wide range of cell types, including germ cells in chimeric mice, both in vitro and in vivo. Androgenetic haploid mouse ESC lines containing only the paternal chromosomes have also been generated by removal of the maternal pronucleus from zygotes and by introduction of sperm into enucleated oocytes (Li et al., 2012; Yang et al., 2012). Thus, pluripotency, self-renewal, and haploidy can be incorporated together in a single cell line.

Li et al. (2014) have successfully extended the zygote-based strategy of androgenetic haploid ESC derivation to the rat, which in many ways is more advantageous than the mouse as an animal model of human physiology, behavior, and disease. Only a few years have passed since the first authentic rat ESCs were isolated, and rat genetic tools have still lagged behind those available for the mouse. Li et al. (2014) found that their newly established rat androgenetic haploid ESCs (RahESCs) are pluripotent and self-renewable and can serve as a “sperm-like” genetic tool (Figure 1A). In

their study, Li et al. engineered the RahESCs by inserting a red fluorescent protein (RFP) marker transgene and targeting deletion of the *Scn4b* gene that has been implicated in human long-QT syndrome. Strikingly, intracytoplasmic injection of the RahESCs into metaphase oocytes, assisted by chemical activation, led to production of fertile rats that inherit the RFP transgene and *Scn4b* deletion. This procedure is termed intracytoplasmic RahESC injection (ICAI) and is reminiscent of the widely used intracytoplasmic sperm injection (ICSI) method, which demonstrates the use of renewable “sperm-like” cells for transgenic rat production. Moreover, RahESCs provide a desired platform for recessive genetic screening, as exemplified by random insertion of gene trap elements into the haploid genome via *piggyBac* (PB) transposons. RahESCs also demonstrated potential multiple-site-specific targeting of three Tet family genes when the authors used the CRISPR-Cas9 system. Both of these procedures ultimately gave rise to homozygous mutants through diploidization.

In the second study, Leeb et al. (2014) clearly demonstrate the power of recessive genetic screening in haploid ESCs (Figure 1B). The self-renewal property of mouse haploid ESCs allows a random mutagenesis screen to identify factors that promote exit from the self-renewal state itself. A haploid reporter ESC line expressing destabilized GFP under the control of the endogenous promoter for *Rex1*, a known marker of pluripotency, has been used to monitor the maintenance of self-renewal. The ESCs were mutagenized by random insertion of PB-based gene-trap transposons and then

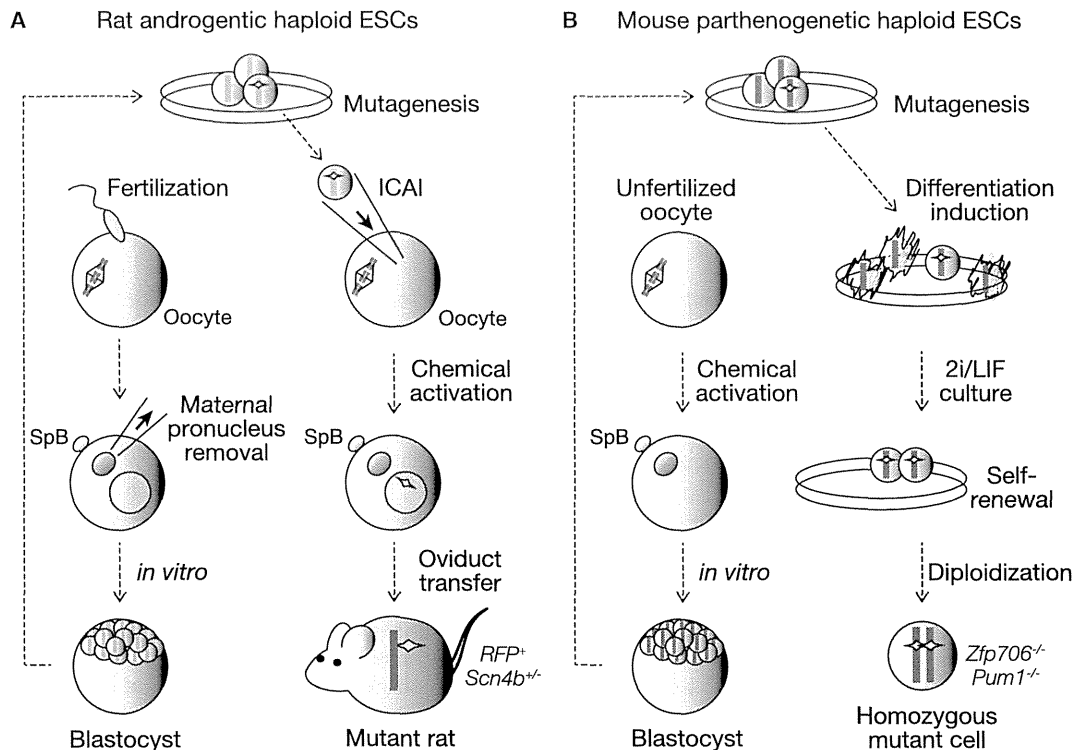


Figure 1. Haploid Embryonic Stem Cell System as a Versatile Genetic Tool in Rodents

(A) Intracytoplasmic rat androgentic haploid ESC injection (ICAI) contributes to production of both transgenic (*RFP⁺*) and knockout (*Scn4b^{+/+}*) mutant rats. (B) Gene-trap mutagenesis of mouse parthenogenetic haploid ESCs allows loss-of-function genetic screening to identify genes (*Zfp706* and *Pum1*) that promote exit from the self-renewal state. Blue and red rectangles represent the paternal and maternal sets of haploid chromosomes, respectively. Yellow stars represent mutations. SpB indicates the second polar body.

cultured in differentiation-permissive conditions. After repetition of the differentiation induction, fractions of GFP-retaining cells were processed for positive selection in the defined 2i/LIF medium, in which only self-renewing stem cells can grow. At the end, the candidate gene-trap mutations responsible for the persistent self-renewal were collectively recovered by deep sequencing. These results provided a proof-of-principle of this elegant approach by isolating known differentiation inducers, including multiple components of the Fgf/Erk and GSK3/Tcf3 signaling pathways. Moreover, the authors identified and validated factors not previously implicated in pluripotent cell biology. These factors included the small zinc finger protein *Zfp706*, which represses the pluripotency factor *Klf4*, and the RNA binding protein *Pum*, which downregulates naive pluripotency circuit genes in a post-transcriptional manner.

Historically, loss-of-function genetic screening has been the most advanced

in yeast because of the availability of efficient methodologies. Therefore, “yeast envy” has motivated mammalian geneticists to develop tools such as the engineered diploid *Blm* mutant ESC line with inducible loss-of-heterozygosity (Horie et al., 2011) and the above-mentioned haploid ESC lines. Most recently, three independent groups have constructed genome-scale single-guide RNA (sgRNA) libraries of the CRISPR-Cas9 system for human (Shaheen et al., 2014; Wang et al., 2014) and mouse (Koike-Yusa et al., 2013) cells. Lentiviral delivery of a library leads to stable integration and expression of sgRNA, mostly resulting in iterative biallelic cleavage of target sites in diploid cells until both alleles lose the target sequences by misrepair. Because the integrated sgRNA sequences serve as DNA barcodes, this type of mutagenesis allows recessive loss-of-function screening for both positive and negative selection. The majority of mutations generated by CRISPR-Cas9-mediated

cleavage are relatively small deletions (<20 bp) and could be insufficient to affect the function of long noncoding genes and other functional elements. Therefore, CRISPR-Cas9 and other mutagenesis systems, including gene trapping in haploid cells, are mutually supportive. The next goal would be to discover two or more genetic components that are codependent on each other, which would correspond to the “synthetic lethal” screening approach that is well developed in yeast. Nevertheless, with a variety of emerging genetic tools, mammalian geneticists are now overcoming their “yeast envy.”

REFERENCES

- Elling, U., Taubenschmid, J., Wirnsberger, G., O'Malley, R., Demers, S.P., Vanhaelen, Q., Shukalyuk, A.I., Schmauss, G., Schramek, D., Schuetgen, F., et al. (2011). *Cell Stem Cell* 9, 563–574.
- Horie, K., Kokubu, C., Yoshida, J., Akagi, K., Isotani, A., Oshitani, A., Yusa, K., Ikeda, R., Huang,

Y., Bradley, A., and Takeda, J. (2011). *Nat. Methods* 8, 1071–1077.

Koike-Yusa, H., Li, Y., Tan, E.P., Velasco-Herrera, M.D.C., and Yusa, K. (2013). *Nat. Biotechnol.* Published online December 23, 2013. <http://dx.doi.org/10.1038/nbt.2800>.

Leeb, M., and Wutz, A. (2011). *Nature* 479, 131–134.

Leeb, M., Dietmann, S., Paramor, M., Niwa, H., and Smith, A. (2014). *Cell Stem Cell* 14, this issue, 385–393.

Li, W., Shuai, L., Wan, H., Dong, M., Wang, M., Sang, L., Feng, C., Luo, G.Z., Li, T., Li, X., et al. (2012). *Nature* 490, 407–411.

Li, W., Li, X., Li, T., Jiang, M.G., Wan, H., Luo, G.Z., Feng, C., Cui, X., Teng, F., Yuan, Y., et al. (2014). *Cell Stem Cell* 14, this issue, 404–414.

Shalem, O., Sanjana, N.E., Hartenian, E., Shi, X., Scott, D.A., Mikkelsen, T.S., Heckl, D., Ebert, B.L., Root, D.E., Doench, J.G., and Zhang, F. (2014). *Science* 343, 84–87.

Wang, T., Wei, J.J., Sabatini, D.M., and Lander, E.S. (2014). *Science* 343, 80–84.

Yang, H., Shi, L., Wang, B.A., Liang, D., Zhong, C., Liu, W., Nie, Y., Liu, J., Zhao, J., Gao, X., et al. (2012). *Cell* 149, 605–617.

Heps with Pep: Direct Reprogramming into Human Hepatocytes

Ludovic Vallier^{1,2,*}

¹Wellcome Trust-Medical Research Council Stem Cell Institute, Anne McLaren Institute for Regenerative Medicine, Department of Surgery, West Forvie Site, Robinson Way, Cambridge CB20SZ, UK

²Wellcome Trust Sanger Institute, Hinxton CB10 1SA, UK

*Correspondence: lv225@cam.ac.uk

<http://dx.doi.org/10.1016/j.stem.2014.02.010>

The limited supply and expansion capacity of primary human hepatocytes presents major challenges for pharmaceutical applications and development of cell-based therapies for liver diseases. Now in *Cell Stem Cell*, two papers demonstrate efficient direct reprogramming of human fibroblasts into induced hepatocytes, which exhibit metabolic properties similar to primary hepatocytes.

The liver is a unique organ that performs a broad spectrum of functions. It stores reserves of iron, vitamins, and minerals and detoxifies alcohol, drugs, and other chemicals that accumulate in the bloodstream. The liver also produces bile, albumin, and blood-clotting factors. Finally, the liver performs an essential metabolic activity by storing glycogen. These tasks are managed by one cell type, the hepatocyte, which constitutes the main cellular unit of the liver. Genetic disorders or injuries that prevent the liver from carrying out these essential activities result in life-threatening diagnosis and end-stage liver diseases that require organ transplantation. Thus, generating large quantities of hepatocytes as an alternative to liver transplants is a major objective for drug development and regenerative medicine. However, freshly isolated hepatocytes come in limited supply, often from donated organs that are of poor quality, and are impossible to expand in large quantities in vitro. Therefore, deriving hepatocytes from stem cell populations such as human pluripotent stem cells (hPSCs) presents an

attractive alternative to primary cells. Now in *Cell Stem Cell*, two studies, from the groups of Lijian Hui and Hongkui Deng, demonstrate an additional approach by directly reprogramming fibroblasts into human induced hepatocytes (hiHeps) (Du et al., 2014; Huang et al., 2014).

hPSCs have been used advantageously to produce hepatocytes for disease modeling (Rashid et al., 2010) and for developmental studies. However, generation of cells displaying all the functional characteristics of mature hepatocytes has been proven difficult. Indeed, hPSC-derived hepatocytes uniformly express fetal markers such as AFP and lack key metabolic activity associated with adult cells such as cytochrome p450, especially CYP3A4. Importantly, recent improvements involving 3D cultures (Ogawa et al., 2013), small molecule screens (Shan et al., 2013), and also in vivo maturation with coculture of endothelial cells (Takebe et al., 2013) have resulted in important functional improvements, including the expression of inducible CYP3A4 and diminished AFP expression.

The development of robust pluripotent stem cell differentiation protocols has been impaired by the lack of knowledge concerning the mechanisms that regulate the functional maturation of the human liver after birth. Direct reprogramming approaches could bypass this last limitation by avoiding the need to mimic a complex path of development in vitro. Accordingly, previous reports have shown that overexpression of Gata4/HNF1alpha/Foxa3 or HNF4a/FoxA1/FoxA2/FoxA3 in mouse embryonic fibroblasts, following genetic ablation of p19, enables the production of induced hepatocyte-like cells (iHep) (Huang et al., 2011; Sekiya and Suzuki, 2011). These cells can be expanded in vitro while displaying a limited metabolic activity, and they retain the capacity to colonize the failing liver of mice lacking fumarylacetoacetate hydrolase (Fah^{-/-}), a common animal model of liver failure (Azuma et al., 2007).

The two reports published in this issue of *Cell Stem Cell* have successfully extended this approach to human fetal cells. Huang et al. (2014) report that overexpression of



ScreenFect™ A による遺伝子導入の特徴

高崎健康福祉大学薬学部 腫瘍生物学研究室 村上 孝

はじめに

プラスミド DNA や siRNA などの機能的な核酸を細胞に導入し、その細胞機能や形態の変化を観察する手法は現代生物医学の最も基本的な技術の一つになっている。分子細胞生物学の成熟に伴い、1990 年代には様々な遺伝子導入技術が開発され、培養細胞のみならず生体組織への遺伝子導入方法にも様々なレベルで開発が及んでいる¹⁾。その結果、安全な各種ウイルスベクター等が開発され、ヒト疾患を対象にした各種遺伝子治療も実践されるようになってきている²⁾。このような先端医療の開発の前には、効率よくウイルスベクターを産生できる技術開発があったからに他ならない。例えば、高効率組み換えレンチウイルスの作製にしても、複数種類のプラスミド DNA を効率よくパッケージング細胞に（非ウイルスベクターとして）導入することが求められる。このことは、機能的な核酸を希望する細胞に安定的に付与できる技術が前提となっていることが伺えよう。本稿では、これまでの筆者らの経験を踏まえ、簡易な手順で培養細胞への遺伝子導入が高い効率で実現できるカチオン性リポフェクション法について紹介したい。

リポフェクション法による遺伝子導入

株化培養細胞への遺伝子導入法としては主に、リン酸カルシウム法、リポフェクション法、DEAE デキストラン法、エレクトロポレーション法、マイクロインジェクション法、ウイルスベクター法などがあり、それぞれの特徴がある（表 1）³⁾。筆者の研究室では、ホタル由来ルシフェラーゼ（firefly: *Photinus pyralis*）を安定的に発現するヒトがん細胞株ライブラリーの作製を行なっている（作製細胞株は [独] 医薬基盤研究所 JCRB 細胞バンクより入手可能: <http://cellbank.nibio.go.jp/cellinfo/luc/>）。その際、レトロ（レンチ）ウイルスベクターを用いた遺伝

表 1. 遺伝子導入方法の種類と特徴³⁾

リン酸カルシウム法	正電荷を持つカルシウムイオンを負の電荷を持つ DNA に結合させ、そこにリン酸を加えると、カルシウムイオンとリン酸が結合して複合体の沈殿が生じる。このリン酸カルシウムと DNA の複合体がエンドサイトーシスによって細胞に取り込まれ、その後、細胞核に移行することにより遺伝子発現に至ると考えられている。特殊な装置や技術を必要とせず、比較的簡単。
リポフェクション法	陽性荷電脂質などからなる脂質二重膜小胞（リポソーム）と導入する DNA との電気的な相互作用により複合体を形成させ、貪食や膜融合により細胞に取り込ませる方法。導入効率が高く、オリゴヌクレオチド、二本鎖 RNA の導入が可能で操作が簡単。特別な装置・設備は不要。
DEAE デキストラン法	本法による動物細胞内への遺伝子の取込みや核内輸送メカニズムは、DEAE デキストランと DNA が複合体を形成して細胞表面に吸着し、エンドサイトーシスによって細胞内へと取り込まれるというモデルが考えられている。リン酸カルシウム法やリポフェクション法にくらべて遺伝子導入効率が低く、細胞毒性がある。
エレクトロポレーション法	高電圧パルスにより一過性に脂質二重層の細胞膜構造を不安定化し、DNA を取り込ませる方法。導入効率は電圧・電気パルスの長さ・温度・細胞および DNA の濃度・バッファー組成の条件により左右される。操作が簡単で遺伝子導入効率が高いが、高価な専用機械が必要。
マイクロインジェクション法	1 個の細胞に微細ガラス注入針を通じて試料を導入する方法。原理は簡単ながら、高度な技術を要する。トランスジェニック動物（マウス、ラットなど）の作製における常道で、受精卵に導入遺伝子を注入する。
ウイルスベクター法	レトロ（レンチ）ウイルス、アデノウイルス、アデノ随伴ウイルスなど、ウイルス固有の生活環を応用し、標的の細胞に感染させ、遺伝子導入する。組み換えウイルスを作製する必要があるため、封じ込めレベルで P2 以上の施設が要求される。

子導入方法を採用しており、組み換えウイルス作製にリポフェクション法を用いている^{4,5)}。効率的なルシフェラーゼ発光細胞を作製するためには、細胞周期（細胞分裂）に依存することなく導入遺伝子が発現する系が有利となる。その観点から、現在ではレンチウイルスベクターを用いている（ベクタープラスミドとして、pLVSiN-CMV-puro に pGL3 由来のルシフェラーゼ [Luc] を組み込んだ pLVSiN-Luc を利用）。高力価の組み換えレンチウイルスを作製するため、パッケージング細胞 293T への導入系から最適化する目的で、各種遺伝子導入法の検討を行なった。24-well plate を用い、

古典的なリン酸カルシウム法に加え、低毒性型リポフェクション試薬として ScreenFect™ A [和光純薬工業コード No. 299-73203] や B 社製品（以下、試薬 B）について pLVSiN-Luc を導入核酸として Luc 活性を指標に試験を行なった（図 1）。ScreenFect™ A や試薬 B では添加試薬によって導入効率が変わるため、その試験も行っている（図 1 A-C）。ScreenFect™ A および試薬 B では添加試薬の量に依存して Luc 活性が大きく変化している（24 時間後）。古典的なリン酸カルシウム法では「pH」によって導入 plasmid DNA を巻き込んだ沈殿形成が大きく変化するが、概ね ScreenFect™ A と同等の

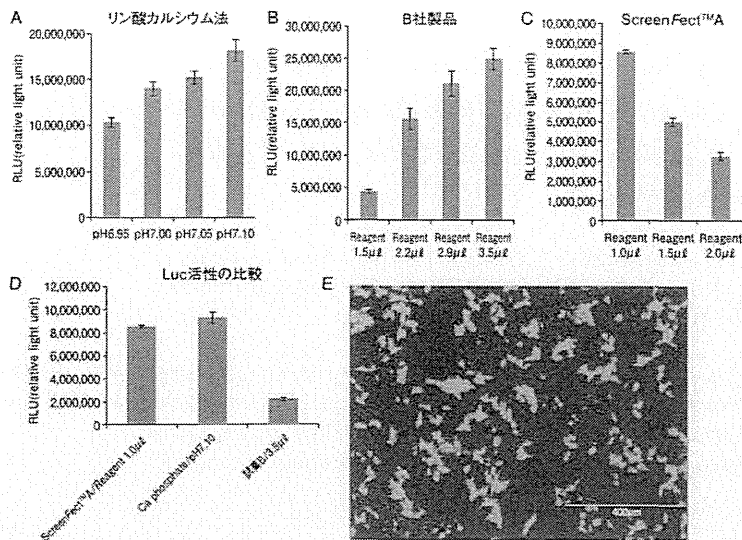


図1. 遺伝子導入試薬による遺伝子発現の差異

- 293T 細胞を Type I コラーゲンでコーティングされた 24-well plate に遺伝子導入の前日に播種し、(A)–(C) の各条件でトランスフェクションを行なった。Luc 活性の測定は 24 時間後に実施した (結果は 3 well の平均)。
- (A) リン酸カルシウム法による pH 条件と Luc 活性。pLVISIN-Luc (1 μg) に終濃度 0.25 M CaCl₂ となるように各 pH 調整された 2×HEPES buffer を添加し、24-well plate に添加した。細胞密度：2.7 × 10⁵ 個 /well。
- (B) 試薬 B と B 社導入促進試薬添加による Luc 活性。pLVISIN-Luc (1 μg) を用い、導入促進試薬 1 μL とした場合に B 社製品を図のように添加した。細胞密度：5 × 10⁵ 個 /well。
- (C) ScreenFect™A による Luc 活性。pLVISIN-Luc (0.3 μg) に ScreenFect™A transfection reagent を図のように添加。細胞密度：2.7 × 10⁵ 個 /well。
- (D) 導入 plasmid DNA を固定した場合の各トランスフェクション法による Luc 活性。細胞密度は各メーカー推奨に設定し、pLVISIN-Luc (0.3 μg) を用いて Luc 活性を計測。
- (E) GFP 発現の代表的な結果。前述の ScreenFect™A を用いて pCAGGS-EGFP (0.3 μg) を導入し、24 時間後に EVOS Cell Imaging System によって描出した。ここでは明視野との重ね合わせのため、GFP 発現量の高い細胞が描出されている (FACS では 100% 陽性)。

高い Luc 活性が得られている (図 1 D)。これらの結果は、個々の試薬によって、導入核酸の量や至適細胞密度などの条件が異なるため、あくまでも一例としてみて頂きたい。

その一方で遺伝子導入効率を推定するため、GFP (green fluorescent protein) を発現する pCAGGS-EGFP を用いて、GFP 陽性細胞について検討を行なった (Tali[®] イメージベースサイトメーターにて計測)。その結果、293T 細胞に対する導入効率はリボ

フェクション試薬 3 種類ではいずれも GFP 陽性率はほぼ 100% であり (24 時間後：図 1 E)、試薬自体による毒性も観察されなかった (図 2 A)。残念ながらリン酸カルシウム法では細胞傷害率が高く、約 70% が Trypan Blue 染色陽性であった (図 2 A)。これらの結果から、24-well plate を用いたアッセイ系では細胞毒性が少なく高い導入効率を実現できる ScreenFect™A の利用価値は高いように思われる。とりわけ、抗生物質や血清を含む培地

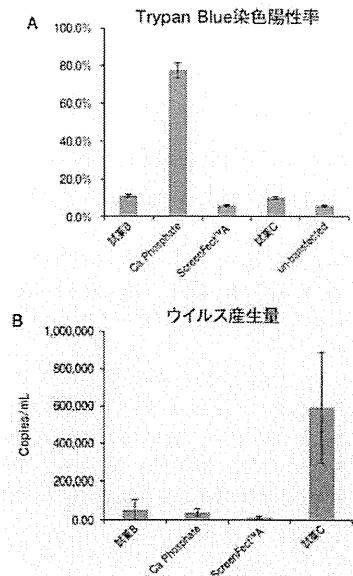


図2. 遺伝子導入による細胞傷害の有無と導入スケールによる遺伝子発現の差異

- (A) 前述の各遺伝子導入に C 社製品 (以下試薬 C) を加え、293T 細胞 (24-well plate) にてトランスフェクションを行なった。24 時間後に Trypan Blue 染色にて評価した (図は陽性率を示す)。
- (B) 前述の各試薬を径 60 mm 培養皿にスケールアップし、pLVISIN-Luc (3 μg) に Packaging mix を加え、組み換えレンチウイルスを作製した。遺伝子導入後 72 時間後に 293T 細胞の培養上清を回収し、レンチウイルス qRT-PCR 迅速タイター測定キットにて RNA titer を測定した。

をそのまま利用することができ、導入後の培地交換を要しない点に簡便さを感じる。

実験スケールによる導入効率の変化

一般的には前述のような pilot 試験を経て、スケールアップを図る実験者は多いと思われる。我々も定石通り、組み換えレンチウイルス産生に向けて ScreenFect™A を用いて 293T 細胞への遺伝子導入系をスケールアップした (径 60mm dish)。その結果、培養上清中に含まれるウイルス産生量を

ORIGINAL ARTICLE: CLINICAL

Epstein–Barr virus-associated T/natural killer-cell lymphoproliferative disorder in children and young adults has similar molecular signature to extranodal nasal natural killer/T-cell lymphoma but shows distinctive stem cell-like phenotype

Siok-Bian Ng^{1,2,3}, Koichi Ohshima⁴, Viknesvaran Selvarajan¹, Gaofeng Huang³, Shoa-Nian Choo¹, Hiroaki Miyoshi⁴, Norio Shimizu⁵, Renji Reghunathan³, Hsin-Chieh Chua⁶, Allen Eng-Juh Yeoh⁶, Thuan-Chong Quah⁶, Liang-Piu Koh⁷, Poh-Lin Tan⁶ & Wee-Joo Chng^{2,3,7}

¹Department of Pathology and ⁷Department of Haematology-Oncology, National University Cancer Institute of Singapore, National University Health System, Singapore, ²Yong Loo Lin School of Medicine and ³Cancer Science Institute of Singapore, National University of Singapore, Singapore, ⁴Department of Pathology, Kurume University, Kurume, Japan, ⁵Department of Virology, Tokyo Medical and Dental University, Tokyo, Japan and ⁶Department of Pediatrics, National University Health System, Singapore

Abstract

We performed gene expression profiling in Epstein–Barr virus (EBV)-associated T/natural killer (NK)-cell lymphoproliferative disorder in children and young adults (TNKLPDC) in order to understand the molecular pathways deregulated in this disease and compared it with nasal-type NK/T-cell lymphoma (NKTL). The molecular and phenotypic signature of TNKLPDC is similar to NKTL, with overexpression of p53, survivin and EZH2. Down-regulation of EZH2 in TNKLPDC cell lines led to an increase in apoptosis and decrease in tumor viability, suggesting that EZH2 may be important for the survival of TNKLPDC cells and hence potentially a useful therapeutic target. Notably, our gene expression profiling revealed a distinctive enrichment of stem cell related genes in TNKLPDC compared to NKTL. This was validated by a significantly higher expression of aldehyde dehydrogenase 1 (ALDH1) in TNKLPDC cell lines compared to NKTL cell lines. The novel discovery of cancer stem cell properties in TNKLPDC has potential therapeutic implications in this group of disorders.

Keywords: EBV+ T/NK LPD in children, molecular signature, cancer stem cell, EZH2

Introduction

Chronic active Epstein–Barr virus (EBV) infection of T/natural killer (NK)-cell type (CAEBV-T/NK) and systemic EBV-positive T-cell lymphoproliferative disease of childhood (STLPDC) are a group of diseases characterized by a systemic EBV-infected, cytotoxic T or NK cell proliferation

[1,2]. According to the 2008 World Health Organization (WHO) classification, STLPDC is defined as a monoclonal disease of EBV-infected T-cells while CAEBV is polyclonal [1]. Since these entities show similar and overlapping clinicopathologic features, they have now been collectively referred to as EBV-associated T/NK lymphoproliferative disorders of childhood and young adults (TNKLPDC) (or EBV-associated T/NK lymphoproliferative disorders in non-immunocompromised hosts) [3–7]. Like many EBV-related T/NK lymphoproliferative diseases, TNKLPDC is prevalent in children and young adults in East Asia, Central and South America and Mexico [1,2].

The precise distinction of TNKLPDC from other EBV-associated T/NK lymphomas occurring in adults, such as nasal-type NK/T cell lymphoma (NKTL), can be notoriously difficult because of significant clinicopathologic overlap. Although classically a disease of childhood and young adults, increasing reports of TNKLPDC in adults have been documented, which may reflect a true increase in adult-onset disease or improved recognition and diagnosis of the disease [5,8,9]. In addition, even though CAEBV is a chronic disease and patients with clonal expansion of EBV-infected T and NK cells may remain stable for years without treatment, a proportion of patients with CAEBV will progress to aggressive lymphomas such as aggressive NK cell leukemia (ANKL) and NKTL [8,9]. Isobe *et al.* recently described seven cases of adult onset CAEBV, which shares common features with pediatric cases but with a poor prognosis, and five of seven patients developed T/NK cell lymphomas and ANKL at a

Correspondence: Siok-Bian Ng, Associate Professor, Department of Pathology, National University Hospital, 5 Lower Kent Ridge Road, Main Building, Level 3, Singapore 119074. Tel: 65-67724709. Fax: 65-67780671. E-mail: patnsb@nus.edu.sgmailto, siok_bian_ng@nuhs.edu.sg. Wee-Joo Chng, Associate Professor, Department of Hematology-Oncology, National University Cancer Institute of Singapore, National University Health System (NUHS), 1E, Kent Ridge Rd, Singapore 119228. Tel: 65-67724612. Fax: 65-67775545. E-mail: mdccwj@nus.edu.sg

Received 23 September 2014; accepted 13 October 2014

1 median of 5 years [9]. Furthermore, patients with NKTL can
2 also present with disseminated disease that becomes indis-
3 tinguishable from TNKLPDC.

4 The molecular abnormalities underlying TNKLPDC and
5 its relationship with NKTL are poorly characterized because
6 TNKLPDC is uncommon, and research on this entity is
7 challenging as most of the tissue biopsies are bone marrow
8 biopsies containing a limited amount of tumor. In this study,
9 we performed, for the first time, gene expression profiling
10 (GEP) on TNKLPDC and compared the signature with that of
11 NKTL obtained in our previous study [10], with the objective
12 of understanding the molecular pathways deregulated in this
13 disease and to determine whether the molecular signature of
14 TNKLPDC is distinct from NKTL.

16 Methods

18 Case selection

19 Patients with a diagnosis of EBV-associated T/NK-cell
20 lymphoproliferative disorder without known underlying
21 immune deficiency were identified from the archives of
22 the Department of Pathology, National University Hospital
23 (NUH) and Kurume University, from 2003 to 2014. Cases
24 were classified according to the 2008 WHO lymphoma
25 classification and nomenclature proposed following the
26 National Institutes of Health (NIH) consensus report in 2008
27 [3]. A total of 22 cases of TNKLPDC with adequate material
28 for work-up and fulfilling the diagnostic criteria were identi-
29 fied. The 22 cases included three cases of chronic active EBV
30 infection of T/NK type (CAEBV), 15 cases of systemic EBV-
31 associated T-cell LPD of childhood (STLPDC) and four cases
32 with features borderline between CAEBV and STLPDC. We
33 considered the presence of an abnormal karyotype and/or
34 monoclonal TCRG gene rearrangement as indicative of a
35 clonal proliferation [2]. The four cases were difficult to classify
36 accurately because of lack of clonality data, which distin-
37 guish between CAEBV (polyclonal) and STLPDC (mono-
38 clonal) as defined by the WHO [1]. The clinicopathological
39 features of the cases are included in Supplementary Table I
40 to be found online at [http://informahealthcare.com/doi/abs/
41 10.3109/10428194.2014.983099](http://informahealthcare.com/doi/abs/10.3109/10428194.2014.983099). Cases of extranodal nasal
42 type NKTL were excluded. Four cases of TNKLPDC with ade-
43 quate formalin-fixed paraffin-embedded (FFPE) tissue and
44 good quality RNA were selected for GEP (cases 5, 7, 16, 17).
45 FFPE control tissues from normal skin and lymph nodes were
46 included. This study was approved by the Domain Specific
47 Review Board of the National Healthcare Group, Singapore.

49 Gene expression profiling and analysis

50 Total RNA from human FFPE tissues was isolated using a High
51 Pure RNA Paraffin Kit (Roche Applied Science, Mannheim,
52 Germany). We conducted genome-wide GEP on TNKLPDC
53 and normal control FFPE samples using an Illumina WG-
54 DASL Assay (Whole Genome cDNA-mediated Annealing,
55 Selection, and Ligation) (Illumina, Inc., San Diego, CA)
56 [11,12]. Raw signals are extracted from Illumina Beadstudio
57 software, and normalized using a linear calibration method,
58 as we have previously described [10]. Analysis of the data was
59 done by R/Bioconductor.

60 In order to determine the similarity in GEP between
61 NKTL and TNKLPDC, we calculated the expression fold-
62 change for each gene as the mean expression of the gene
63 in TNKLPDC samples and mean expression in normal
64 samples. We plotted this fold-change between TNKLPDC
65 and normal versus the fold-change between NKTL and nor-
66 mal (obtained from our previous study) [10] to determine
67 the degree of Pearson correlation. To determine the genes
68 specific to TNKLPDC in comparison to NKTL and normal
69 tissues, we first selected genes with more than two-fold
70 change between TNKLPDC and normal tissues, which con-
71 stituted the candidate list of differentially expressed genes
72 in TNKLPDC. Then using significance analysis of microar-
73 rays (SAM) [13] we generated another list of genes that was
74 abnormally expressed between TNKLPDC and NKTL, with
75 cut-off fold-change > 2 and p -value < 0.01 . The intersection
76 of the above two lists resulted in a final list of genes that
77 were abnormally expressed specifically in TNKLPDC com-
78 pared to NKTL and normal tissues.

80 Immunohistochemistry

81 In order to validate the expression of p53, survivin and EZH2
82 in the tumor and not the non-neoplastic population, we per-
83 formed the following double stains: CD3/p53, CD3/survivin
84 and CD3/EZH2, on 4 μ m tissue sections of TNKLPDC sam-
85 ples using a Leica BondMax auto-stainer, and conditions are
86 listed in Supplementary Table II to be found online at [http://
87 informahealthcare.com/doi/abs/10.3109/10428194.2014.
88 983099](http://informahealthcare.com/doi/abs/10.3109/10428194.2014.983099). Appropriate positive tissue controls were used. The
89 immunohistochemical (IHC) expression of all the antibodies
90 was scored as a percentage of the tumor cell population by
91 one of the authors (S.-B.N.), without knowledge of the clini-
92 copathologic and GEP data. For p53 and survivin antibodies,
93 positive expression was defined as nuclear staining in 10%
94 or more of the tumor population, as previously described
95 [10]. For EZH2 antibody, positive expression was defined as
96 nuclear staining in 25% or more of the tumor population, as
97 previously described [14].

99 TNKLPDC and NKTL cell line culture for ALDH analysis and 100 DZNep treatment

101 Six NKTL cell lines (NK-92, HANK-1, NK-YS, SNK-1, SNK-6,
102 SNT-8) and five TNKLPDC cell lines (KAI-3, SNK-10, SNT-13,
103 SNT-15, SNT-16) were used in this study. NK-92 was pur-
104 chased from the American Type Culture Collection (ATCC).
105 HANK-1 was obtained as a kind gift from Dr. Y. Kagami, NK-YS
106 and KAI-3 were from Dr. Y. L. Kwong while SNK-1, SNK-6,
107 SNT-8, SNK-10, SNT-13, SNT-15 and SNT-16 were from Dr.
108 N. Shimizu. Please refer to Supplementary Table III to be
109 found online at [http://informahealthcare.com/doi/abs/
110 10.3109/10428194.2014.983099](http://informahealthcare.com/doi/abs/10.3109/10428194.2014.983099) for cell line culture conditions
111 and Supplementary Table IV to be found online at [http://
112 informahealthcare.com/doi/abs/10.3109/10428194.2014.
113 983099](http://informahealthcare.com/doi/abs/10.3109/10428194.2014.983099) for clinical, phenotypic and genotypic features of the
114 TNKLPDC and NKTL cell lines.

116 ALDH analysis on NKTL and TNKLPDC cell lines

117 An ALDEFUOR kit (Stem Cell Technologies, Durham,
118 NC) was used to examine the aldehyde dehydrogenase

1 (ALDH) enzymatic activity in NKTL and TNKLPDC
 2 cell lines. A single cell suspension was prepared in
 3 ALDEFLUOR assay buffer containing ALDH substrate.
 4 As negative controls, each sample was treated with
 5 diethylaminobenzaldehyde (DEAB), a specific ALDH
 6 inhibitor. This resulted in a significant decrease in the
 7 fluorescence intensity of ALDH+ cells and was used to
 8 identify ALDH+ cells. The amount of intracellular fluores-
 9 cence was measured using a BD LSR II (Becton Dickinson,
 10 San Diego, CA) flow cytometer and analyzed using BD
 11 FACSDiva™ software.

13 **Treatment of TNKLPDC cell lines with DZNep**

14 Exponentially growing cells of KAI-3, SNK-10, SNT-15 and
 15 SNT-16 cell lines were treated with the respective concentra-
 16 tions of an inhibitor of EZH2 (DZNep), and dimethylsul-
 17 foxide (DMSO) (0.1%) treated cell lines served as vehicle
 18 controls. Treated cells were diluted in phosphate buffered
 19 saline (PBS), sonicated and then pelleted by centrifugation
 20 at 300g for 5 min. The cell pellet was then resuspended in
 21 lysis buffer with a cocktail of protease inhibitors (Promega,
 22
 23

Madison, WI). Protein detection by Western blot was done
 to confirm the expression of EZH2 protein after treatment
 with DZNep by electrophoretic transfer of equal amounts
 of sodium dodecyl sulfate-polyacrylamide gel electropho-
 resis (SDS-PAGE) separated proteins to polyvinylidene
 fluoride (PVDF) membranes (Bio-Rad, Hercules, CA), then
 incubation with the respective primary antibodies: EZH2
 (Cell Signaling Tech. Inc., Danvers, MA) and β-actin control
 (Santa Cruz, Dallas, TX), followed by exposure to horserad-
 ish peroxidase (HRP)-conjugated secondary antibodies
 (Santa Cruz) and detection using chemiluminescence (GE
 Healthcare, Uppsala, Sweden).

Apoptotic cell death analyses were carried out follow-
 ing DZNep treatment using Annexin-V-allophycocyanin
 (APC) and propidium iodide (PI) detection systems.
 Following treatment of cells with respective concentra-
 tions of DZNep and DMSO (0.1%) as vehicle controls and
 incubation for 72 h, the cells were collected and washed
 in PBS. The staining of apoptotic cells by Annexin-V-APC
 was assayed using an APC Annexin-V Apoptosis Detection
 Kit (BD Pharmingen, San Jose, CA) according to the

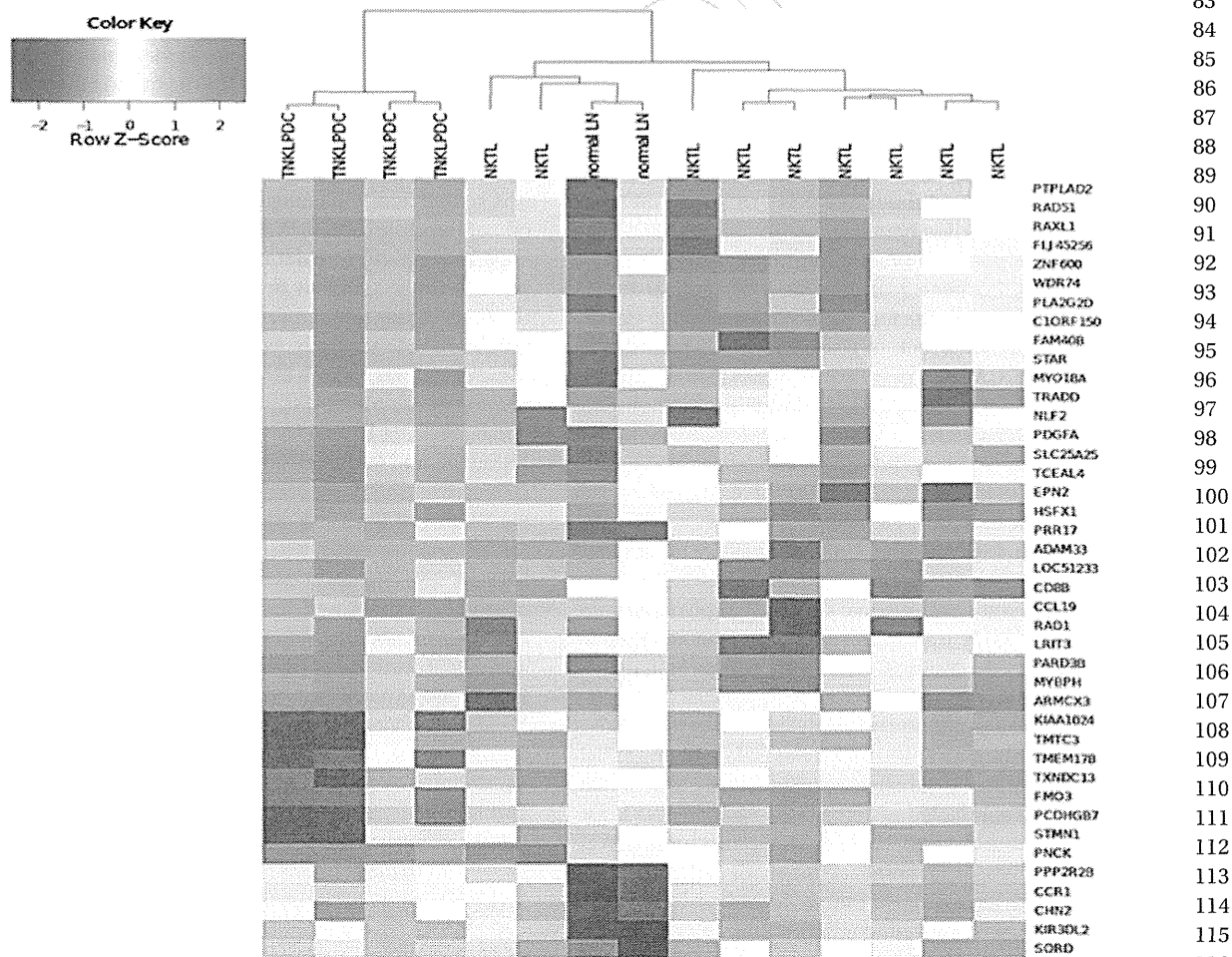


Figure 1. Heatmap showing differentially expressed genes between EBV-associated T/NK lymphoproliferative disorder in children (TNKLPDC) and nasal-type NK/T-cell lymphoma (NKTL). normal LN, normal lymph node.

mono for print colour online

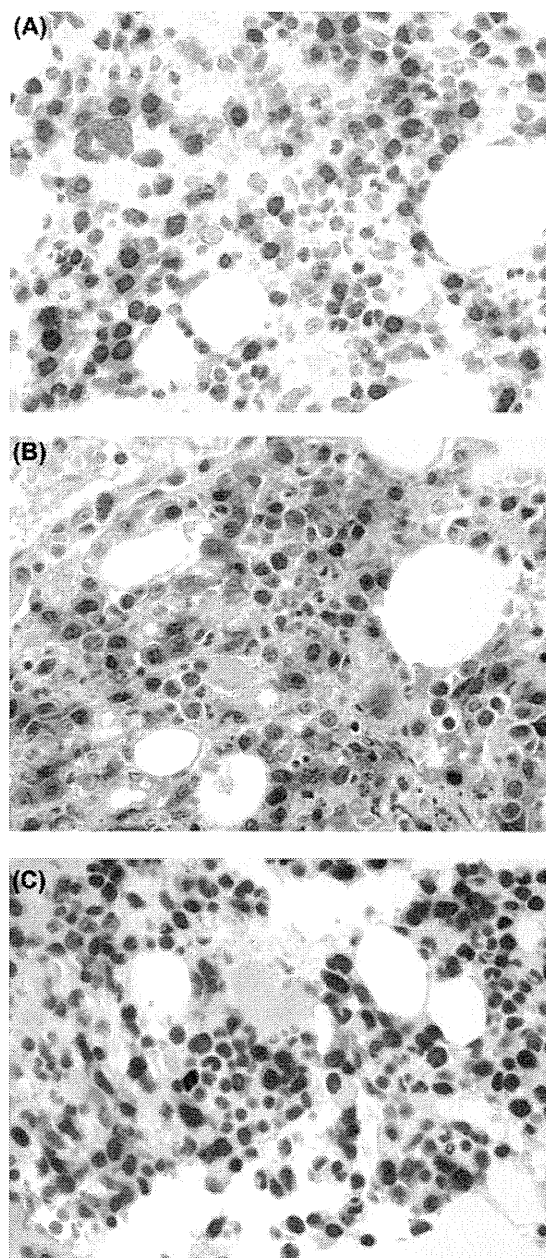


Figure 2. Overexpression of EZH2, p53 and survivin in cases of TNKLPDC. Immunohistochemistry reveals overexpression of EZH2 in case 19 (A, EZH2/CD3 double stain, EZH2 stains nucleus brown and CD3 stains cell membrane/cytoplasm red, original magnification $\times 600$), p53 in case 15 (B, p53/CD3 double stain, p53 stains nucleus brown and CD3 stains cell membrane/cytoplasm red, original magnification $\times 600$) and survivin in case 18 (C, survivin/CD3 double stain, survivin stains nucleus brown and CD3 stains cell membrane/cytoplasm red, original magnification $\times 600$). All photographs were taken with a DP20 Olympus camera (Olympus, Tokyo, Japan) using an Olympus BX41 microscope (Olympus). Images were acquired using a DP Controller 2002 (Olympus) and processed using Adobe Photoshop version 5.5 (Adobe Systems, San Jose, CA).

manufacturer's instructions, and the analysis was performed on a BD LSR II (Becton Dickinson) flow cytometer, using BD FACSDiva™ software.

Results

Gene expression profiling revealed a similar molecular signature between NKTL and TNKLPDC with up-regulation of p53, survivin and EZH2 in TNKLPDC

We performed GEP on four cases of TNKLPDC and compared it to the signature of NKTL that we obtained in our previous study. The expression fold-change for each gene between TNKLPDC versus normal and the expression fold-change of each gene between NKTL versus normal (obtained from our previous study) [10] showed a significant correlation, with Pearson correlation coefficient $r = 0.692$, $p < 2.2 \times 10^{-16}$, indicating a high degree of similarity between TNKLPDC and NKTL (Supplementary Figure 1 to be found online at <http://informahealthcare.com/doi/abs/10.3109/10428194.2014.983099>). Only a small number of genes were significantly differentially expressed between TNKLPDC and NKTL. There were 41 genes showing two-fold or greater difference in expression between TNKLPDC and NKTL, of which 28 were up-regulated and 13 were down-regulated in TNKLPDC compared to NKTL (Figure 1).

Since TNKLPDC shares a similar signature with NKTL at the molecular level, we investigated whether a few of the oncoproteins (p53, survivin and EZH2), which were identified by us to be up-regulated in NKTL in our previous study, are similarly up-regulated in TNKLPDC [10,14]. Indeed, using IHC double stains for p53/CD3, survivin/CD3 and EZH2/CD3, we also found overexpression of p53, survivin and EZH2 in 69% (11/16 cases), 63% (10/16 cases) and 65% (13/20 cases) of our cases of TNKLPDC, respectively, supporting that NKTL and TNKLPDC share similar phenotypic and molecular signatures and hence indirectly validating our GEP results (Figure 2) (Supplementary Table V to be found online at <http://informahealthcare.com/doi/abs/10.3109/10428194.2014.983099> for IHC results for p53, survivin and EZH2).

Inhibition of EZH2 by DZNep induced growth inhibition and apoptosis of TNKLPDC cell lines

We previously reported the overexpression of EZH2 in NKTL, and depletion of EZH2 using a PRC2 inhibitor, DZNep, significantly inhibited the growth of NK tumor cells [14]. Hence, we also treated the TNKLPDC cell lines with DZNep [15,16]. Our results demonstrated that DZNep effectively and dose dependently reduced protein levels of EZH2 in KAI-3, SNK-10, SNT-15 and SNT-16 cell lines [Figure 3(A)], resulting in reduction of cell viability [Figure 3(B)] and an increase in apoptosis as detected by Annexin-V analysis using flow cytometry, in a dose-dependent manner [Figure 3(C)] (Supplementary Figure 2 to be found online at <http://informahealthcare.com/doi/abs/10.3109/10428194.2014.983099> shows increased apoptosis following DZNep treatment).

TNKLPDC is enriched for gene sets associated with hematopoietic and leukemic stem cells compared to NKTL

Despite the similarity of the molecular signature between TNKLPDC and NKTL, we investigated whether there are subtle differences between them. To achieve this, we performed gene set enrichment analysis (GSEA). Using a

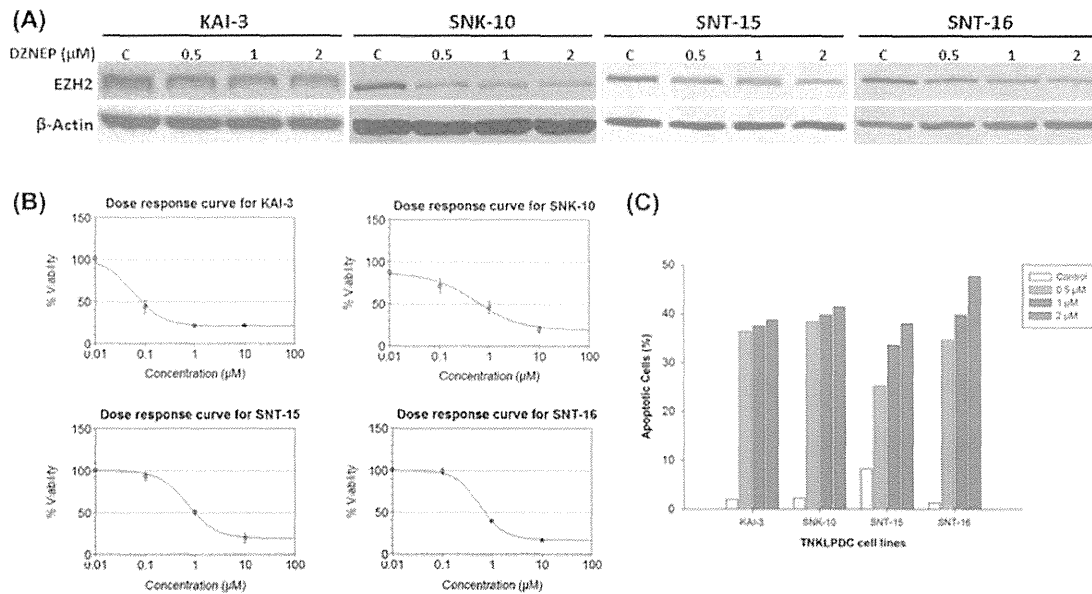


Figure 3. Treatment with DZNep results in a dose-dependent decrease in cellular protein levels of EZH2 in KAI-3, SNK-10, SNT-15 and SNT-16 cell lines (A) and a corresponding reduction in cell viability (B) and increase in apoptosis (C) as detected by flow cytometry.

cut-off false discovery rate of < 20%, we identified 17 gene sets enriched in genes down-regulated in TNKLPDC compared to NKTL (negative enrichment score). Amongst the 17 gene sets, several gene sets of genes down-regulated in stem cells were negatively enriched in TNKLPDC compared to NKTL, meaning that genes down-regulated in stem cells are also down-regulated in TNKLPDC compared to NKTL. This suggests that TNKLPDC shares some molecular feature with stem cells. On the other hand, gene sets of genes up-regulated in invasive/advanced malignancies were negatively enriched in TNKLPDC compared to NKTL, meaning that they are also up-regulated in NKTL compared to TNKLPDC. In other words, NKTL shows up-regulation of genes in invasive tumors and hence shares molecular features with invasive/advanced cancers (Table 1) compared to TNKLPDC (Supplementary Figure 3 to be found online at <http://informahealthcare.com/doi/abs/10.3109/10428194.2014.983099> shows GSEA enrichment plots of gene sets related to stem cell and invasive/advanced cancers which are negatively enriched in TNKLPDC compared to NKTL). This result is consistent with the different clinical presentation of the two malignancies, with TNKLPDC having a leukemic presentation characterized by bone marrow involvement and cytopenias, and NKTL, in contrast, manifesting mostly as aggressive solid cancers.

To further verify that TNKLPDC may have a more stem cell related phenotype based on the GSEA results, we performed ALDH1 assay in six NKTL cell lines (NK-YS, NK-92, HANK-1, SNK-1, SNK-6, SNT-8) and five TNKLPDC cell lines (KAI-3, SNK-10, SNT-13, SNT-15, SNT-16). ALDH enzymes are a family of intracellular enzymes that participate in cellular detoxification, differentiation and drug resistance through the oxidation of cellular aldehydes [17]. ALDH1-positive cell populations are capable of generating tumor xenografts [18], and ALDH1 is used as a marker of cancer stem cells

(CSCs) [19]. The proportion of ALDH1-positive cells in both TNKLPDC and NKTL cell lines ranged from 0.2% to 10.2%, in line with reports that leukemic stem cells constitute only a subfraction of the blast cell population [20,21]. In agreement with the GSEA result, there was a significant difference in ALDH1 expression in TNKLPDC compared to NKTL cell lines, with median of 8.15% of cells expressing ALDH1 in TNKLPDC compared to 2.4% in NKTL ($p = 0.04$), suggesting that there was a higher proportion of tumor cells with CSC properties in TNKLPDC compared to NKTL [Figures 4(A) and 4(B)]. Interestingly, the SNK-1 cell line, derived from a 24-year-old patient with TNKLPDC (CAEBV) who subsequently developed NKTL, also demonstrated a higher level of ALDH1 expression compared to cell lines derived from patients with NKTL without a history of TNKLPDC.

Discussion

TNKLPDC is a group of poorly understood lymphoproliferative disorders in children and young adults, which can be difficult to distinguish from the disseminated form of NKTL. The pathobiology is poorly characterized, and the disease is often aggressive with no effective treatment. Various therapies have been tried for the treatment of CAEBV, including antiviral, chemotherapeutic and immunomodulatory drugs, with only limited success. These regimens are not effective in achieving sustainable complete remission, and hematopoietic stem cell transplant (HSCT) seems to be the only curative therapy for CAEBV at present [8].

We report, for the first time, that TNKLPDC shows a similar molecular signature to NKTL. Furthermore, a number of oncoproteins that we have previously shown to be overexpressed in NKTL, such as p53, EZH2 and survivin, are similarly overexpressed in TNKLPDC. This is not unexpected, as both entities are characterized by an

1 Table I. Gene sets differentially enriched between TNKLPDC and NKTL showing 17 gene sets that are negatively enriched in TNKLPDC compared to NKTL. 60

2

3 Name	Description	Size of gene sets	Enrichment score	FDR <i>q</i> -value	61
4 VECCHI_GASTRIC_CANCER_ADVANCED_VS_EARLY_UP*	Up-regulated genes distinguishing between two subtypes of gastric cancer: advanced (AGC) and early (EGC)	19	-0.7683091	0	62
5 GAL_LEUKEMIC_STEM_CELL_DN†	Genes down-regulated in leukemic stem cells (LSCs), defined as CD34 + CD38- [Gene ID = 947, 952] cells from patients with AML (acute myeloid leukemia) compared to CD34 + CD38+ cells	61	-0.5313042	0.00122956	63
6 LU_TUMOR_VASCULATURE_UP	Genes up-regulated in endothelial cells derived from invasive ovarian cancer tissue	6	-0.927103	0.05146535	64
7 RUIZ_TNC_TARGETS_DN	Genes down-regulated in T98G cells (glioblastoma) by TNC [Gene ID = 3371].	26	-0.5973733	0.05591349	65
8 DAVICIONI_TARGETS_OF_PAX_FOXO1_FUSIONS_DN	Genes down-regulated in RD cells (embryonal rhabdomyosarcoma, ERMS) by expression of PAX3- or PAX7-FOXO1 [Gene ID = 5077, 5081, 2308] fusions off retroviral vectors	10	-0.7663204	0.05456302	66
9 POOLA_INVASIVE_BREAST_CANCER_UP*	Genes up-regulated in atypical ductal hyperplastic tissues from patients with (ADHC) breast cancer vs. those without the cancer (ADH)	62	-0.4721814	0.08633608	67
10 JAATINEN_HEMATOPOIETIC_STEM_CELL_DN†	Genes down-regulated in CD133+ [Gene ID = 8842] cells (hematopoietic stem cells, HSCs) compared to CD133- cells	56	-0.4827268	0.07452668	68
11 TURASHVILI_BREAST_LOBULAR_CARCINOMA_VS_LOBULAR_NORMAL_UP*	Genes up-regulated in lobular carcinoma vs. normal lobular breast cells.	13	-0.6917861	0.09243327	69
12 SCHUETZ_BREAST_CANCER_DUCTAL_INVASIVE_UP*	Genes up-regulated in invasive ductal carcinoma (IDC) relative to ductal carcinoma <i>in situ</i> (DCIS, non-invasive)	58	-0.4718207	0.08723507	70
13 AKL_HTLV1_INFECTION_DN	Genes down-regulated in WE17/10 cells (CD4+ [Gene ID = 920] T lymphocytes) infected by HTLV1 (and thus displaying low CD7 [Gene ID = 924]) compared to uninfected (i.e. CD7+) cells	10	-0.7377943	0.12973607	71
14 SANA_RESPONSE_TO_IFNG_DN	Genes down-regulated in five primary endothelial cell types (lung, aortic, iliac, dermal, and colon) by IFNG [Gene ID = 3458].	10	-0.7334317	0.11817111	72
15 LEE_LIVER_CANCER_MYC_E2F1_UP	Genes up-regulated in hepatocellular carcinoma (HCC) from MYC and E2F1 [Gene ID = 4609, 1869] double transgenic mice	14	-0.6603344	0.12351392	73
16 TAKEDA_TARGETS_OF_NUP98_HOXA9_FUSION_3D_DN†	Genes down-regulated in CD34+ [Gene ID = 947] hematopoietic cells by expression of NUP98-HOXA9 fusion [Gene ID = 4928, 3205] off a retroviral vector at 3 days after transduction	9	-0.7459078	0.13656901	74
17 VERHAAK_AML_WITH_NPM1_MUTATED_UP	Genes up-regulated in patients with acute myeloid leukemia (AML) with mutated NPM1 [Gene ID = 4869]	58	-0.452349	0.13712986	75
18 MCCLUNG_CREB1_TARGETS_DN	Genes down-regulated in the nucleus accumbens (a major reward center in the brain) 8 weeks after induction of CREB1 [Gene ID = 1385] expression in a transgenic Tet-Off system	6	-0.848532	0.15731472	76
19 SMID_BREAST_CANCER_RELAPSE_IN_BONE_UP*	Genes up-regulated in bone relapse of breast cancer	16	-0.6191868	0.1730245	77
20 MCLACHLAN_DENTAL_CARIES_DN	Genes down-regulated in pulpal tissue extracted from carious teeth	57	-0.4333106	0.17132571	78

21 TNKLPDC, Epstein-Barr virus-associated T/natural killer-cell lymphoproliferative disorder in children and young adults; NKTL, extranodal nasal natural killer/T-cell lymphoma; FDR, false discovery rate.

22 *Gene sets of genes up-regulated in invasive/advanced malignancies.

23 †Gene sets of genes down-regulated in stem cells.

24 EBV-associated cytotoxic T/NK proliferation and share similar clinical features.

25 Despite the similarity, there are some subtle differences in the molecular profile. Our GESA data revealed a distinctive enrichment of stem cell related genes in TNKLPDC compared to NKTL. Indeed, the expression of ALDH1, a marker of stem cell properties, was significantly higher in TNKLPDC compared

24 to NKTL cell lines, and this supports the validity of our GESA result. On the other hand, genes overexpressed in advanced malignancies were enriched in NKTL. This result is consistent with the different clinical presentation of the two malignancies, with TNKLPDC having a leukemic presentation characterized by bone marrow involvement and cytopenias, and NKTL, in contrast, manifesting as aggressive solid cancers.

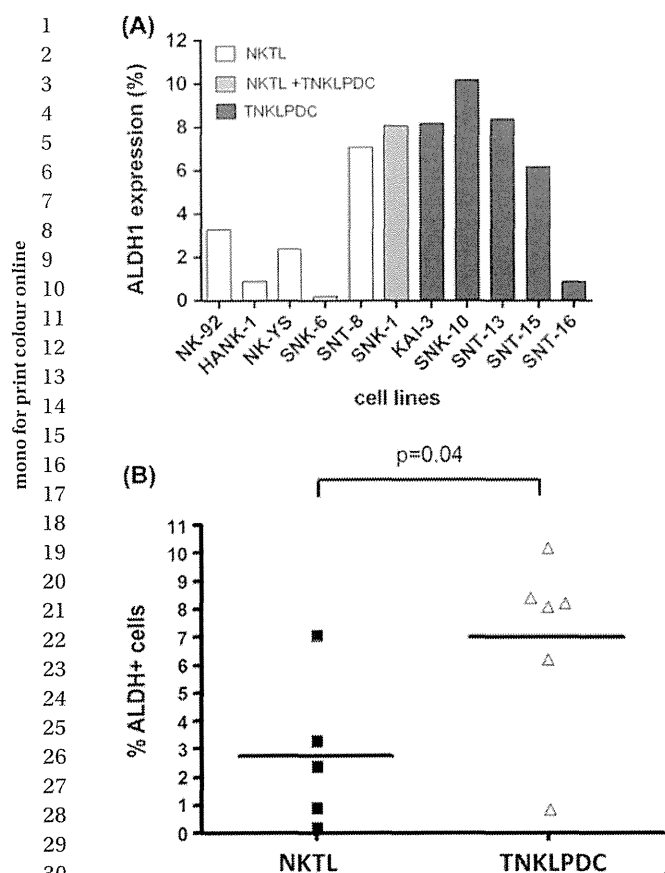


Figure 4. (A) TNKLPDC cell lines show a higher proportion of cells expressing ALDH1 compared to NKTL cell lines. (B) TNKLPDC cell lines show a significantly higher proportion of cells expressing ALDH1 compared to NKTL cell lines (median expression of 8.15% vs. 2.4%, $p = 0.04$).

The CSC hypothesis proposes that tumors arise from a subset of cells (usually representing the minority population) with distinctive stem cell properties characterized by the ability to undergo self-renewal, proliferation and multipotential differentiation [22,23]. A role for CSCs has been characterized for acute leukemias [24], and CSCs also exist in solid tumors, including brain, breast and colon [25]. In acute myeloid leukemia, only a subfraction of cells are proposed to be leukemia stem cells (LSCs), while the majority of cells are either transitional cells with limited proliferative capacity or more differentiated end cells [21]. In general, these CSCs are quiescent and resistant to conventional chemotherapy that usually targets proliferating cells. Hence, our discovery of potential CSC properties in TNKLPDC cell lines has important therapeutic implications in this group of disorders. In addition, this may also explain the success of allogeneic HSCT in the treatment of TNKLPDC [26–28] and why conventional chemotherapy, without HSCT, is often unsuccessful in the treatment of TNKLPDC.

Although HSCT at present appears to be curative for patients with CAEBV, it is not without life-threatening complications. In this regard, identification of new therapeutic strategies and targets is greatly needed. Importantly, we demonstrated EZH2 to be aberrantly overexpressed

in TNKLPDC. EZH2 is a H3K27-specific histone methyltransferase and a component of the polycomb repressive complex 2 (PRC2), which plays a key role in the epigenetic maintenance of the repressive chromatin mark and has been implicated to play an oncogenic role in cancers [29]. Our *in vitro* studies using DZNep, a compound capable of inhibiting EZH2 by depleting PRC2 components [15], showed that successful down-regulation of EZH2 in four TNKLPDC cell lines led to a significant increase in apoptosis and decrease in the viability of tumor cells. Although DZNep is not a specific inhibitor of EZH2 and may affect other molecules [30], our results suggest that EZH2 may be important for survival of TNKLPDC cells, and down-regulation/degradation of EZH2 could be a potential therapeutic strategy in TNKLPDC. This is of interest, as EZH2 inhibitors are currently being developed for clinical use [31,32].

In conclusion, our study showed that the molecular and phenotypic signature of TNKLPDC is similar to NKTL, with overexpression of p53, survivin and EZH2. Down-regulation of EZH2 results in an increase in apoptosis and reduction in cell viability, supporting the rationale for targeting EZH2 as a potential therapeutic strategy in the treatment of NKTL. In addition, the novel discovery of potential CSC properties in TNKLPDC cell lines has important therapeutic implications in this group of disorders, although this finding requires further validation in primary tumor samples in a larger cohort of patients.

Acknowledgements

S.-B.N. is supported by a National University Health System Clinician Scientist Program award. This work was partially supported by a grant from the Ministry of Education (MOE) Academic Research Fund (AcRF) Tier 1 (WBS No. R-179-000-046-112).

W.-J.C. is supported by a NMRC Clinician Scientist Investigator award. This work was partially supported by a Singapore Cancer Syndicate Grant, and the National Research Foundation Singapore and Singapore Ministry of Education under the Research Centers of Excellence initiative.

Potential conflict of interest: Disclosure forms provided by the authors are available with the full text of this article at www.informahealthcare.com/lal.

References

- Quintanilla-Martinez L, Kimura H, Jaffe ES. EBV-positive T-cell lymphoproliferative disorders of childhood. In: Swerdlow SH, Campo E, Harris NL, et al., editors. WHO classification of tumours of haematopoietic and lymphoid tissues. 4th ed. Lyon: IRAC Press; 2008. pp 278–280.
- Ko YH, Jaffe ES. Epstein-Barr virus-positive systemic T-lymphoproliferative disorders and related lymphoproliferations of childhood. In: Jaffe ES, Harris NL, Vardiman JW, et al., editors. Hematopathology. Philadelphia, PA: Elsevier Saunders; 2011. pp 492–505.
- Cohen JI, Kimura H, Nakamura S, et al. Epstein-Barr virus-associated lymphoproliferative disease in non-immunocompromised hosts: a status report and summary of an international meeting, 8–9 September 2008. *Ann Oncol* 2009;20:1472–1482.

[4] Kimura H, Ito Y, Kawabe S, et al. EBV-associated T/NK-cell lymphoproliferative diseases in nonimmunocompromised hosts: prospective analysis of 108 cases. *Blood* 2012;119:673-686.

[5] Ohshima K, Kimura H, Yoshino T, et al. Proposed categorization of pathological states of EBV-associated T/natural killer-cell lymphoproliferative disorder (LPD) in children and young adults: overlap with chronic active EBV infection and infantile fulminant EBV T-LPD. *Pathol Int* 2008;58:209-217.

[6] Wang RC, Chang ST, Hsieh YC, et al. Spectrum of Epstein-Barr virus-associated T-cell lymphoproliferative disorder in adolescents and young adults in Taiwan. *Int J Clin Exp Pathol* 2014;7:2430-2437.

[7] Hong M, Ko YH, Yoo KH, et al. EBV-positive T/NK-cell lymphoproliferative disease of childhood. *Korean J Pathol* 2013;47:137-147.

[8] Fujiwara S, Kimura H, Imadome K, et al. Current research on chronic active Epstein-Barr virus infection in Japan. *Pediatr Int* 2014;56:159-166.

[9] Isobe Y, Aritaka N, Setoguchi Y, et al. T/NK cell type chronic active Epstein-Barr virus disease in adults: an underlying condition for Epstein-Barr virus-associated T/NK-cell lymphoma. *J Clin Pathol* 2012;65:278-282.

[10] Ng SB, Selvarajan V, Huang G, et al. Activated oncogenic pathways and therapeutic targets in extranodal nasal-type NK/T cell lymphoma revealed by gene expression profiling. *J Pathol* 2010;223:496-510.

[11] Fan JB, Yeakley JM, Bibikova M, et al. A versatile assay for high-throughput gene expression profiling on universal array matrices. *Genome Res* 2004;14:878-885.

[12] Bibikova M, Talantov D, Chudin E, et al. Quantitative gene expression profiling in formalin-fixed, paraffin-embedded tissues using universal bead arrays. *Am J Pathol* 2004;165:1799-1807.

[13] Tusher VG, Tibshirani R, Chu G. Significance analysis of microarrays applied to the ionizing radiation response. *Proc Natl Acad Sci USA* 2001;98:5116-5121.

[14] Yan J, Ng SB, Tay JL, et al. EZH2 overexpression in natural killer/T-cell lymphoma confers growth advantage independently of histone methyltransferase activity. *Blood* 2013;121:4512-4520.

[15] Tan J, Yang X, Zhuang L, et al. Pharmacologic disruption of Polycomb-repressive complex 2-mediated gene repression selectively induces apoptosis in cancer cells. *Genes Dev* 2007;21:1050-1063.

[16] Xie Z, Bi C, Cheong LL, et al. Determinants of sensitivity to DZNep induced apoptosis in multiple myeloma cells. *PLoS One* 2011;6:e21583.

[17] Moreb J, Schweder M, Suresh A, et al. Overexpression of the human aldehyde dehydrogenase class I results in increased

resistance to 4-hydroperoxycyclophosphamide. *Cancer Gene Ther* 1996;3:24-30.

[18] Huang EH, Hynes MJ, Zhang T, et al. Aldehyde dehydrogenase 1 is a marker for normal and malignant human colonic stem cells (SC) and tracks SC overpopulation during colon tumorigenesis. *Cancer Res* 2009;69:3382-3389.

[19] Liang D, Shi Y. Aldehyde dehydrogenase-1 is a specific marker for stem cells in human lung adenocarcinoma. *Med Oncol* 2012;29:633-639.

[20] Hwang K, Park CJ, Jang S, et al. Flow cytometric quantification and immunophenotyping of leukemic stem cells in acute myeloid leukemia. *Ann Hematol* 2012;91:1541-1546.

[21] Kummermehr JC. Tumour stem cells—the evidence and the ambiguity. *Acta Oncol* 2001;40:981-988.

[22] Dick JE. Stem cell concepts renew cancer research. *Blood* 2008;112:4793-4807.

[23] Jordan CT. Cancer stem cell biology: from leukemia to solid tumors. *Curr Opin Cell Biol* 2004;16:708-712.

[24] Hope KJ, Jin L, Dick JE. Human acute myeloid leukemia stem cells. *Arch Med Res* 2003;34:507-514.

[25] Ailles LE, Weissman IL. Cancer stem cells in solid tumors. *Curr Opin Biotechnol* 2007;18:460-466.

[26] Gotoh K, Ito Y, Shibata-Watanabe Y, et al. Clinical and virological characteristics of 15 patients with chronic active Epstein-Barr virus infection treated with hematopoietic stem cell transplantation. *Clin Infect Dis* 2008;46:1525-1534.

[27] Sato E, Ohga S, Kuroda H, et al. Allogeneic hematopoietic stem cell transplantation for Epstein-Barr virus-associated T/natural killer-cell lymphoproliferative disease in Japan. *Am J Hematol* 2008;83:721-727.

[28] Kawa K, Sawada A, Sato M, et al. Excellent outcome of allogeneic hematopoietic SCT with reduced-intensity conditioning for the treatment of chronic active EBV infection. *Bone Marrow Transplant* 2011;46:77-83.

[29] Chang CJ, Hung MC. The role of EZH2 in tumour progression. *Br J Cancer* 2012;106:243-247.

[30] Miranda TB, Cortez CC, Yoo CB, et al. DZNep is a global histone methylation inhibitor that reactivates developmental genes not silenced by DNA methylation. *Mol Cancer Ther* 2009;8:1579-1588.

[31] McCabe MT, Ott HM, Ganji G, et al. EZH2 inhibition as a therapeutic strategy for lymphoma with EZH2-activating mutations. *Nature* 2012;492:108-112.

[32] Knutson SK, Wigle TJ, Warholc NM, et al. A selective inhibitor of EZH2 blocks H3K27 methylation and kills mutant lymphoma cells. *Nat Chem Biol* 2012;8:890-896.

Supplementary material available online

Supplementary Tables I-V and Figures 1-3 showing further data.

PROOF

Supplementary material for Ng S-B, et al. Epstein-Barr virus-associated T/natural killer-cell lymphoproliferative disorder in children and young adults has similar molecular signature to extranodal nasal natural killer/T-cell lymphoma but shows distinctive stem cell-like phenotype, *Leukemia & Lymphoma*, 2014; doi: 10.3109/10428194.2014.983099.

Supplementary Table I. Clinical data of 22 cases of TNKLPDC.

No	Diagnosis*	Sex	Ethnicity	Age (yrs)	Tissue type	GEP	Treatment	Follow up	TCR PCR	BM karyotype
1	CAEBV	M	Indonesian	3.4	BM	No	HLH -P	Alive	PC	N
2	CAEBV	M	Chinese	13.1	BM	No	HLH-P, AHCT	Dead (AHCT complications)	PC	N
3	CAEBV	M	Vietnamese	24.8	BM	No	Chemo	Alive	PC	N
4	STLPDC	F	Chinese	5.3	BM	No	HLH-P, AHCT	Alive	MC	N
5	STLPDC	M	Chinese	1.4	Skin	Yes	HLH-P, AHCT	Alive (graft rejection)	MC	N
6	STLPDC	F	Indonesian	6.1	BM	No	HLH-P	Alive	MC	N
7	STLPDC	M	Chinese	16.7	LN	Yes	Steroids, AHCT	Dead	MC	N
8	CAEBV vs STLPDC	M	Japanese	4	liver	No	AHCT	Alive	NA	NA
9	CAEBV vs STLPDC	F	Japanese	19	BM	No	AHCT	Alive	NA	NA
10	CAEBV vs STLPDC	F	Japanese	19	BM	No	Chemo	Alive	NA	NA
11	CAEBV vs STLPDC	F	Japanese	39	Skin	No	Chemo	Dead	NA	NA
12	STLPDC	F	Vietnamese	16.4	BM	No	HLH-P	Dead	MC	Abn
13	STLPDC	F	Chinese	4.8	BM	No	HLH-P	Alive	MC	N
14	STLPDC	M	Indonesian	13.3	BM	No	HLH -P	Dead	MC	Abn
15	STLPDC	M	Indonesian	20.9	BM	No	HLH -P	Dead	MC	Abn
16	STLPDC	F	Chinese	9.5	LN	Yes	Supportive	Dead	PC	Abn
17	STLPDC	M	Chinese	18.7	LN	Yes	HLH -P	Dead	MC	N
18	STLPDC	M	Vietnamese	1	BM	No	HLH-P	NA	MC	Mosaic
19	STLPDC	M	Filipino	7.6	BM	No	HLH-P	Dead	NA	N
20	STLPDC	F	Chinese	19.3	BM	No	HLH-P	Dead	PC	Abn
21	STLPDC	F	Japanese	48	BM	No	Chemo, AHCT	Dead	NA [‡]	NA
22	favour STLPDC	M	Others	18.3	BM	No	Supportive	Dead	NA	NA

Abbreviations: M, male; F, female; NA, not available; BM, bone marrow; LN, lymph node; CAEBV, chronic active EBV infection of T-NK type, STLPDC; systemic EBV+ T cell lymphoproliferative disorder of childhood; GEP, gene expression profiling; HLH-P, 2004 Histiocytic Lymphohistiocytosis protocol; AHCT, Allogeneic hematopoietic cell transplant; Chemo, chemotherapy; TCR, T cell receptor gamma gene rearrangement; PC, polyclonal; MC, monoclonal; N, normal; abn, abnormal.

[‡] EBV terminal repeats analysis revealed monoclonality.

* based on WHO classification and recommendation from NIH consensus meeting in 2008 [1,2].

Supplementary Table II. Summary of immunohistochemical double stains conditions.

Antibody	Source	Clone	Dilution	Retrieval	Incubation	Chromogen
EZH2/CD3	EZH2: Novocastra	6A10	1:200	ER1-20'	15'	DAB
	CD3: DAKO	Polyclonal	1:70	ER2-20'	15'	AP
P53/CD3	P53: DAKO	D0-7	1:100	ER2-20'	15'	DAB
	CD3: DAKO	Polyclonal	1:50	-	15'	AP
Survivin/CD3	Survivin: Cell Signalling	7G4B7E	1:75	ER1-20'	15'	DAB
	CD3: DAKO	Polyclonal	1:50	ER2-20'	15'	AP

DAB, diaminobenzidine (brown stain); AP, alkaline phosphatase (red stain).

Supplementary Table III. Culture conditions of TNKLPDC and NKTL cell lines.

Cell Line	Description of Disease	Cytokine Dependency	Culture Conditions
NK-92	NHL-LGL (adult)	IL-2	α -MEM ² 12.5% Fetal Bovine Serum ⁵ 12.5% Horse Serum ⁵ 100 U/ml IL-2 ⁶
HANK-1	NKTL	IL-2	COSMEDIUM 001 ³ 10% Human Serum ⁵ 100 U/ml IL-2 ⁶
NK-YS	NKTL	IL-2	RPMI-1640 ¹ 10% Fetal Bovine Serum ⁵ 100 U/ml IL-2 ⁶
SNK-1	NKTL	IL-2	Artemis 2 ⁴ 2% Human Serum ⁵ 700 U/ml IL-2 ⁶
SNK-6	NKTL	IL-2	Artemis 2 ⁴ 2% Human Serum ⁵ 700 U/ml IL-2 ⁶
SNT-8	NKTL	IL-2	Artemis 2 ⁴ 2% Human Serum ⁵ 700 U/ml IL-2 ⁶
KAI-3	TNKLPDC	IL-2	RPMI-1640 ¹ 10% Fetal Bovine Serum ⁵ 100 U/ml IL-2 ⁶
SNK-10	TNKLPDC	IL-2	Artemis 2 ⁴ 2% Human Serum ⁵ 700 U/ml IL-2 ⁶
SNT-13	TNKLPDC	IL-2	Artemis 2 ⁴ 2% Human Serum ⁵ 700 U/ml IL-2 ⁶
SNT-15	TNKLPDC	IL-2	Artemis 2 ⁴ 2% Human Serum ⁵ 700 U/ml IL-2 ⁶
SNT-16	TNKLPDC	IL-2	Artemis 2 ⁴ 2% Human Serum ⁵ 700 U/ml IL-2 ⁶

NHL-LGL, Non-Hodgkin lymphoma with large granular cells; NKTL, nasal-type NK/T cell lymphoma; TNKLPDC, T/NK-cell lymphoproliferative disorders 1, Life Technologies, Carlsbad, CA, USA; ², Stemcell Technologies, USA; ³, Cosmo Bio, Japan; ⁴, Nihon Techno Service, Japan; ⁵, PAA Labs, Austria; ⁶, Miltenyi Biotec, Germany.

Supplementary Table IV. Clinical, phenotypic and genotypic features of TNKLPDC and NKTL cell lines.

Cell line	Sex	Age	Ethnicity	Original description of disease	sample	CD56	EBV	lineage
NK-92	M	50	Caucasian	NHL-LGL (adult)	PB	+	+	NK
SNT-8	F	48	Japanese	NKTL	nasal	+	+	$\gamma\delta$ T
SNK-6	M	62	Japanese	NKTL	nasal	+	+	NK
NK-YS	F	19	Japanese	NKTL	PB	+	+	NK
HANK-1	F	46	Japanese	NKTL	LN	+	+	NK
SNK-1	F	24	Japanese	NKTL with CAEBV	PB	+	+	NK
KAI3	M	13	Japanese	MBH	PB	+	+	NK
SNK-10	M	17	Japanese	CAEBV	PB	+	+	NK
SNT-13	F	13	Japanese	CAEBV	PB	ND	+	$\gamma\delta$ T
SNT-15	F	15	Japanese	CAEBV	PB	ND	+	$\gamma\delta$ T
SNT-16	F	13	Japanese	CAEBV	PB	ND	+	$\alpha\beta$ T

NHL-LGL, Non-Hodgkin lymphoma with large granular cells; NKTL, nasal-type NK/T-cell lymphoma; MBH, mosquito bite hypersensitivity (part of spectrum of EBV+ T/NK lymphoproliferative disease of children and young adult); CAEBV, chronic active EBV infection; PB, peripheral blood; LN, lymph node.

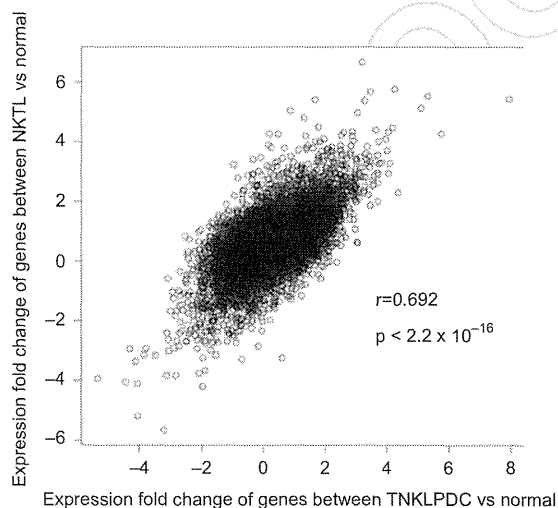
Supplementary Table V. Immunohistochemistry results for p53, survivin and EZH2 in TNKLPDC cases.

Case No.	p53 score (%)	Survivin score (%)	EZH2 score (%)
1	1	1	2
2	7	6	75
3	1	1	NA
4	10	20	22
5	5	1	NA
6	30	85	50
7	32	73	10
8	NA	NA	3
9	NA	NA	28
10	NA	NA	21
11	NA	NA	2
12	90	90	74
13	80	85	85
14	90	9	95
15	90	1	87
16	95	95	90
17	12	85	29
18	47	80	80
19	98	90	85
20	NA	NA	20
21	NA	NA	47
22	7	80	40

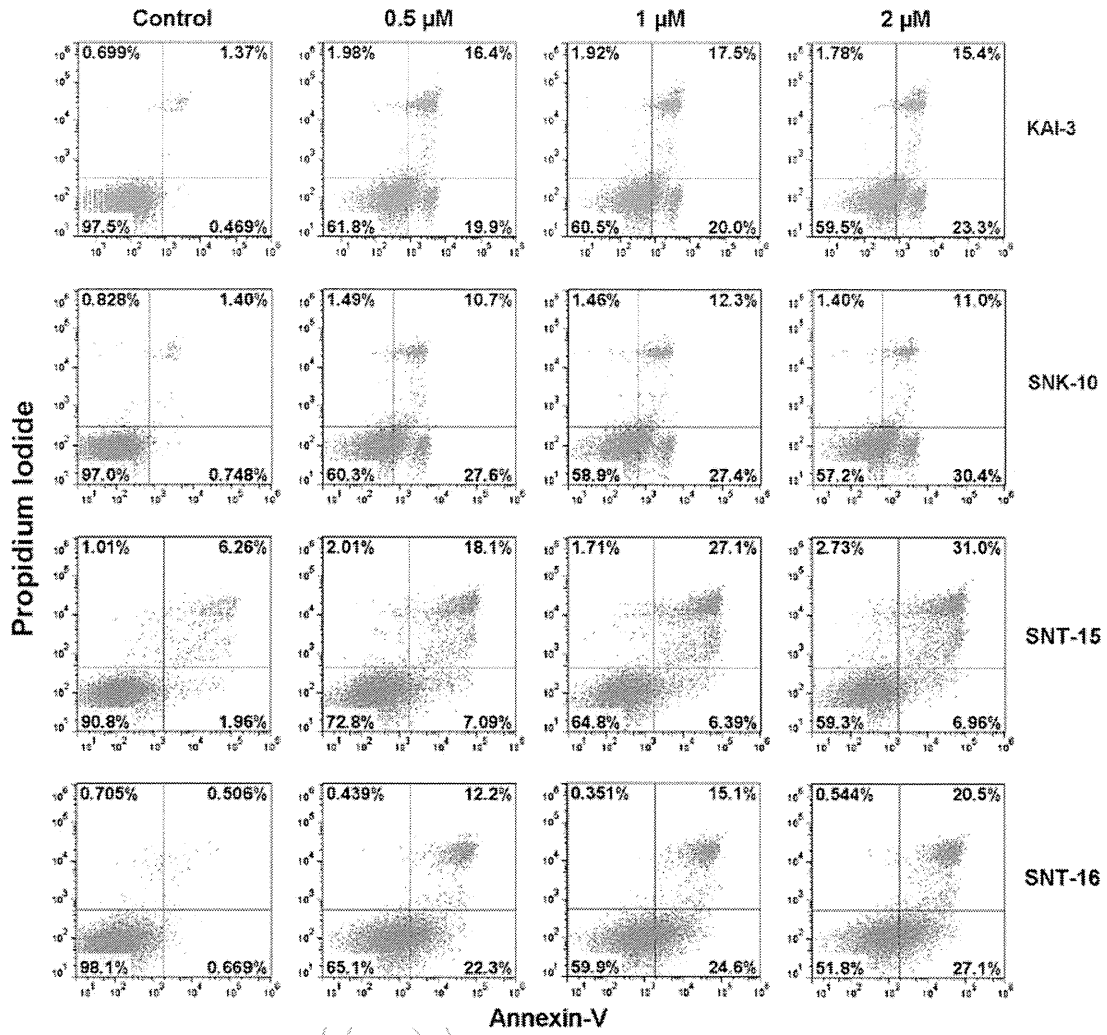
Abbreviations: NA = not available.

References

- [1] Quintanilla-Martinez L, Kimura H, Jaffe ES. EBV-positive T-cell lymphoproliferative disorders of childhood. In: Swerdlow SH, Campo E, Harris NL, et al., editors. *WHO classification of tumours of haematopoietic and lymphoid tissues*. 4th ed. Lyon: IRAC Press; 2008. p 278-280.
- [2] Cohen JI, Kimura H, Nakamura S, Ko YH, Jaffe ES. Epstein-Barr virus-associated lymphoproliferative disease in non-immunocompromised hosts: a status report and summary of an international meeting, 8-9 September 2008. *Ann Oncol* 2009;20:1472-1482.

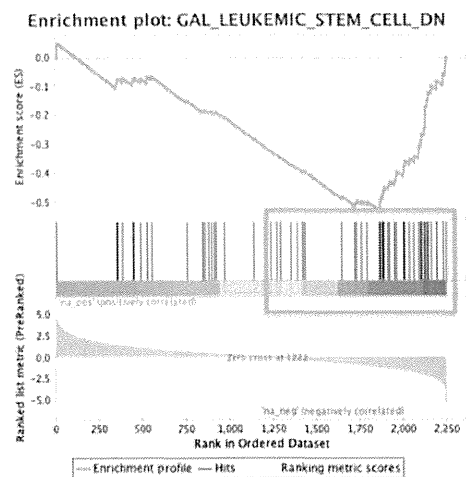


Supplementary Figure 1. Gene expression profiling showed a similar molecular signature between TNKLPDC and NKTL. Scatterplot of the expression fold-change for each gene between TNKLPDC vs Normal and the expression fold-change of each gene between NKTL vs Normal showed a significant correlation with Pearson correlation $r = 0.692$, $p < 2.2 \times 10^{-16}$, indicating a high degree of similarity between TNKLPDC and NKTL.

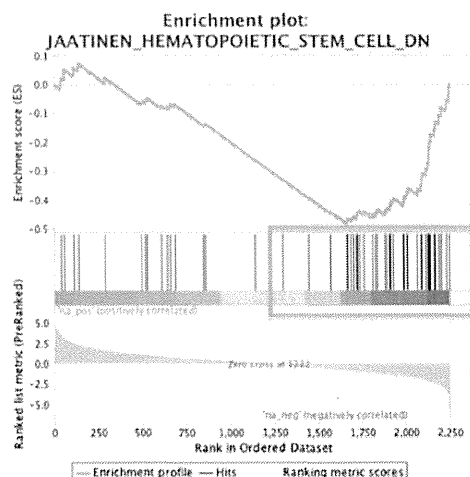


Supplementary Figure 2. Inhibition of EZH2 by DZNep results in dose dependent increase in apoptosis of KAI3, SNK-10, SNT-15 and SNT-16 cell lines detected by flow cytometry using Annexin-V-APC and propidium iodide (PI) assay.

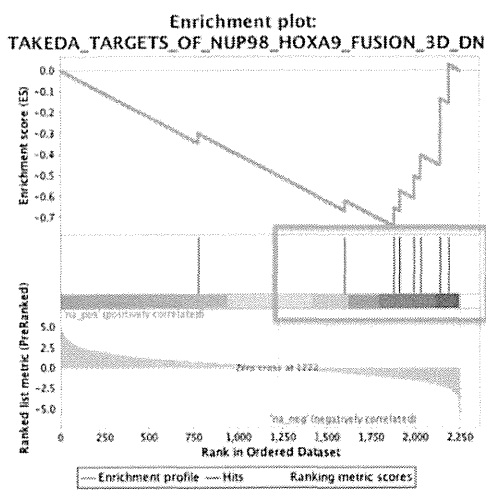
PRO



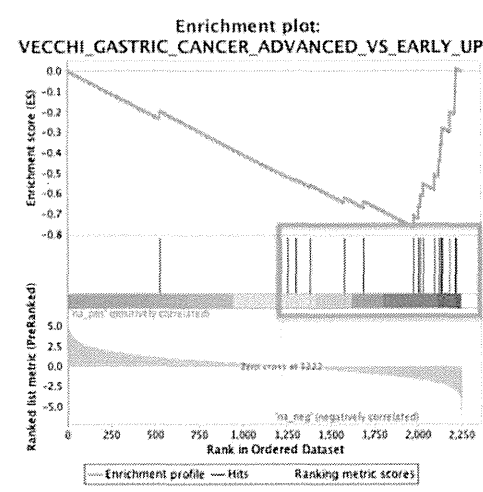
Genes with higher expression in TNKLPDC compared to NKTL Genes with lower expression in TNKLPDC compared to NKTL



Genes with higher expression in TNKLPDC compared to NKTL Genes with lower expression in TNKLPDC compared to NKTL

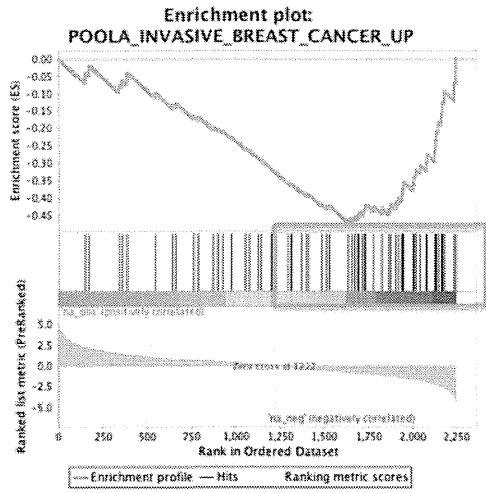


Genes with higher expression in TNKLPDC compared to NKTL Genes with lower expression in TNKLPDC compared to NKTL

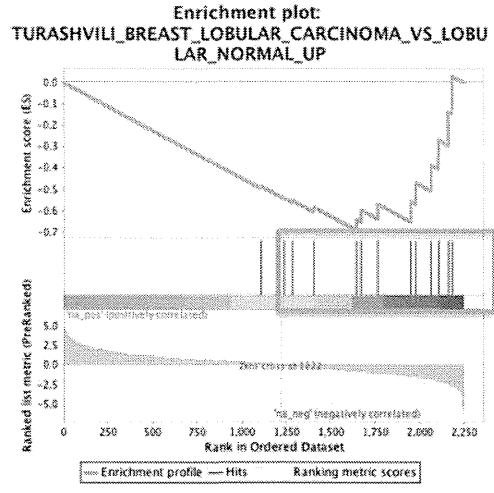


Genes with higher expression in TNKLPDC compared to NKTL Genes with lower expression in TNKLPDC compared to NKTL

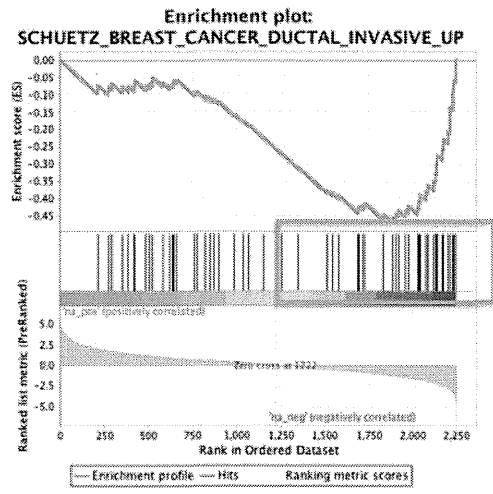
Supplementary Figure 3. GESA enrichment plots showing genesets related to stem cell and invasive/advanced cancers negatively enriched in TNKLPDC compared to NKTL.



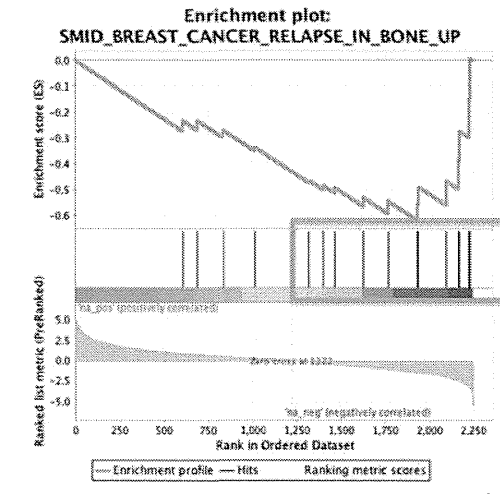
Genes with higher expression in TNKLPDC compared to NKTL Genes with lower expression in TNKLPDC compared to NKTL



Genes with higher expression in TNKLPDC compared to NKTL Genes with lower expression in TNKLPDC compared to NKTL



Genes with higher expression in TNKLPDC compared to NKTL Genes with lower expression in TNKLPDC compared to NKTL



Genes with higher expression in TNKLPDC compared to NKTL Genes with lower expression in TNKLPDC compared to NKTL

Blue box refers to genes downregulated in stem cells are also downregulated in TNKLPDC compared to NKTL implying TNKLPDC has more stem cell like features than NKTL

Pink box refers to genes upregulated in invasive/advanced cancers are also downregulated in TNKLPDC compared to NKTL implying NKTL shares molecular features with invasive/advanced cancers compared to TNKLPDC

Supplementary Figure 3. (Continued)



CD137 Expression Is Induced by Epstein-Barr Virus Infection through LMP1 in T or NK Cells and Mediates Survival Promoting Signals

Mayumi Yoshimori^{1,2}, Ken-Ichi Imadome³, Honami Komatsu^{1,2}, Ludan Wang¹, Yasunori Saitoh⁴, Shoji Yamaoka⁴, Tetsuya Fukuda¹, Morito Kurata⁵, Takatoshi Koyama², Norio Shimizu⁶, Shigeyoshi Fujiwara³, Osamu Miura¹, Ayako Arai^{1*}

1 Department of Hematology, Graduate School of Medical and Dental Sciences, Tokyo Medical and Dental University, Tokyo, Japan, **2** Department of Laboratory Molecular Genetics of Hematology, Graduate School of Health Care Sciences, Tokyo Medical and Dental University, Tokyo, Japan, **3** Department of Infectious Diseases, National Research Institute for Child Health and Development, Tokyo, Japan, **4** Department of Molecular Virology, Graduate School of Medical and Dental Sciences, Tokyo Medical and Dental University, Tokyo, Japan, **5** Department of Comprehensive Pathology, Graduate School of Medical and Dental Sciences, Tokyo Medical and Dental University, Tokyo, Japan, **6** Department of Virology, Division of Medical Science, Medical Research Institute, Tokyo Medical and Dental University, Tokyo, Japan

Abstract

To clarify the mechanism for development of Epstein-Barr virus (EBV)-positive T- or NK-cell neoplasms, we focused on the costimulatory receptor CD137. We detected high expression of *CD137* gene and its protein on EBV-positive T- or NK-cell lines as compared with EBV-negative cell lines. EBV-positive cells from EBV-positive T- or NK-cell lymphoproliferative disorders (EBV-T/NK-LPDs) patients also had significantly higher *CD137* gene expression than control cells from healthy donors. In the presence of IL-2, whose concentration in the serum of EBV-T/NK-LPDs was higher than that of healthy donors, CD137 protein expression was upregulated in the patients' cells whereas not in control cells from healthy donors. *In vitro* EBV infection of MOLT4 cells resulted in induction of endogenous CD137 expression. Transient expression of *LMP1*, which was enhanced by IL-2 in EBV-T/NK-LPDs cells, induced endogenous *CD137* gene expression in T and NK-cell lines. In order to examine *in vivo* CD137 expression, we used EBV-T/NK-LPDs xenograft models generated by intravenous injection of patients' cells. We identified EBV-positive and CD8-positive T cells, as well as CD137 ligand-positive cells, in their tissue lesions. In addition, we detected CD137 expression on the EBV infected cells from the lesions of the models by immunofluorescent staining. Finally, CD137 stimulation suppressed etoposide-induced cell death not only in the EBV-positive T- or NK-cell lines, but also in the patients' cells. These results indicate that upregulation of CD137 expression through LMP1 by EBV promotes cell survival in T or NK cells leading to development of EBV-positive T/NK-cell neoplasms.

Citation: Yoshimori M, Imadome K-I, Komatsu H, Wang L, Saitoh Y, et al. (2014) CD137 Expression Is Induced by Epstein-Barr Virus Infection through LMP1 in T or NK Cells and Mediates Survival Promoting Signals. PLoS ONE 9(11): e112564. doi:10.1371/journal.pone.0112564

Editor: Joseph S. Pagano, The University of North Carolina at Chapel Hill, United States of America

Received: April 22, 2014; **Accepted:** October 20, 2014; **Published:** November 19, 2014

Copyright: © 2014 Yoshimori et al. This is an open-access article distributed under the terms of the Creative Commons Attribution License, which permits unrestricted use, distribution, and reproduction in any medium, provided the original author and source are credited.

Funding: This work was supported by a grant from the Ministry of Health, Labor, and Welfare of Japan (H22-Nanchi-080) as well as a grant from the Ministry of Education, Culture, Sports, Science, and Technology of Japan (23591375). The funders had no role in study design, data collection and analysis, decision to publish, or preparation of the manuscript.

Competing Interests: The authors have declared that no competing interests exist.

* Email: ara.hema@tmd.ac.jp

Introduction

Epstein-Barr virus (EBV) infection can be found in lymphoid malignancies not only of B-cell lineage, but also of T- or NK-cell lineages. These EBV-positive T or NK-cell neoplasms, such as extranodal NK/T-cell lymphoma nasal type (ENKL), aggressive NK-cell leukemia (ANKL), and EBV-positive T- or NK-cell lymphoproliferative diseases (EBV-T/NK-LPDs), are relatively rare but lethal disorders classified as peripheral T/NK-cell lymphomas according to the WHO classification of tumors of hematopoietic and lymphoid malignancies. ENKL is a rapidly progressive lymphoma characterized by extranodal lesions with vascular damage and severe necrosis accompanied by infiltration of neoplastic NK or cytotoxic T cells [1]. ANKL is a markedly aggressive leukemia with neoplastic proliferation of NK cells [2]. EBV-T/NK-LPDs is a fatal disorder presenting sustained infectious mononucleosis-like symptoms, hypersensitivity to mos-

quito bites, or hydroa vacciniforme-like eruption accompanied by clonal proliferation of EBV-infected cells [3,4]. Because most reported cases were children or young adults, and were mainly of the T-cell-infected type, the disorders were designated "EBV-positive T-cell lymphoproliferative diseases of childhood" in the WHO classification, although adult and NK-cell types have been reported [4–6]. The common clinical properties of EBV-T/NK-neoplasms are the presence of severe inflammation, resistance to chemotherapy, and a marked geographic bias for East Asia and Latin America, suggesting a genetic context for disease development [4]. Since these EBV-T/NK-neoplasms overlap [4], common mechanisms are thought to exist in the background and contribute to disease development.

It is well known that EBV infects B cells and makes the infected cells immortal resulting in B-cell lymphomas. Similarly it is suspected that EBV may also cause T- or NK-cell neoplasms. However, why and how EBV latently infects T or NK cells,